J|A|C|S
ARTICLES
Published on Web 06/14/2003

Structural Effects on Encapsulation As Probed in Redox-Active Core Dendrimer Isomers

Tyson L. Chasse, Rakesh Sachdeva, Qun Li, Zemin Li, Randall J. Petrie, and Christopher B. Gorman*

Contribution from the Department of Chemistry, North Carolina State University, Box 8204, Raleigh, North Carolina 27695-8204

Received April 7, 2003; E-mail: chris_gorman@ncsu.edu

Abstract: Three pairs of isomeric, iron−sulfur core dendrimers were prepared. Each isomer pair was distinguished by a 3,5-aromatic substitution pattern (extended) versus 2,6-aromatic substitution pattern (backfolded). Several observations were made that supported the hypothesis that the iron−sulfur cluster cores were encapsulated more effectively in the backfolded isomers as compared to their extended isomeric counterparts. The backfolded isomers were more difficult to reduce electrochemically, consistent with encapsulation in a more hydrophobic microenvironment. Furthermore, heterogeneous electron-transfer rates for the backfolded molecules were attenuated compared to the extended molecules. From diffusion measurements obtained by pulsed field gradient spin−echo NMR and chronoamperometry, the backfolded dendrimers were found to be smaller than the extended dendrimers. Comparison of longitudinal proton relaxation (T_1) values also indicated a smaller, more compact dendrimer conformation for the backfolded architectures. These findings indicated that the dendrimer size was not the major factor in determining electron-transfer rate attenuation. Instead, the effective electron-transfer distance, as determined by the relative core position and mobility in a dendrimer, is most relevant for encapsulation.

Introduction

Encapsulating a functional moiety within a dendrimer leads to several novel properties. These include modulation of the rate and driving force for electron transfer, attenuation of the rates of luminescence quenching, and modulation of catalytic behaviors of the core.[1−4] It is still unclear, however, how the primary structure of the dendrimer biases its conformation and how the conformation of the dendrimer influences these encapsulation behaviors.

Redox-active core dendrimers are particularly suited to study dendritic encapsulation. We recently showed how rates of electron transfer could be varied in iron−sulfur cluster core dendrimers that alternatively contained flexible and rigid linkages.[5] The paramagnetic nature of the iron−sulfur cluster could also be used to elucidate features of the dendrimer conformation via NMR relaxation measurements.[6] The distance of electron transfer and the material surrounding the core governs electron-transfer rate. This distance can be changed by increasing the mass of the dendrons and/or altering the dendron architecture, thereby biasing the dendrimer conformation to increase encapsulation around the redox-active core moiety. The processes that control rate and driving force for electron transfer were also found to differ substantially between dendrimers in solution and in thin film form.[7] The shielded redox unit also can be used to study behaviors relevant to metalloprotein mimicry[1−3,8−11] and charge trapping in molecular electronics.[2,12]

A decisive way to probe the influence of structure on encapsulation via conformation is through the study of constitutional isomers. The synthesis[13,14] and study of dendrimer isomers has had some precedent including the study of linear versus hyperbranched structures,[15,16] supramolecular organization of different dendrimer isomers,[17] stereoisomers in dendrimers (e.g., cis vs. trans azobenzene or stilbene linkages in dendrimers),[18−25] and isomeric metallodendrimers.[26] Recently,

(1) Gorman, C.; Smith, J. C. *Acc. Chem. Res.* **2001**, *34*, 60−71.
(2) Cameron, C. S.; Gorman, C. B. *Adv. Funct. Mater.* **2002**, *12*, 17−20.
(3) Fréchet, J. M. J.; Hecht, S. *Angew. Chem., Int. Ed. Engl.* **2001**, *40*, 74−91.
(4) Astruc, D.; Chardac, F. *Chem. Rev.* **2001**, *101*, 2991−3023.
(5) Gorman, C. B.; Smith, J. C.; Hager, M. W.; Parkhurst, B. L.; Sierzputowska-Gracz, H.; Haney, C. A. *J. Am. Chem. Soc.* **1999**, *121*, 9958−9966.
(6) Gorman, C. B.; Hager, M. W.; Parkhurst, B. L.; Smith, J. C. *Macromolecules* **1998**, *31*, 815−822.
(7) Gorman, C.; Smith, J. C. *J. Am. Chem. Soc.* **2000**, *122*, 9342−9343.
(8) Dandliker, P. J.; Diederich, F.; Gross, M.; Knobler, C. B.; Louati, A.; Sanford, E. M. *Angew. Chem., Int. Ed. Engl.* **1994**, *33*, 1739−1741.
(9) Collman, J. P.; Fu, L.; Zingg, A.; Diederich, F. *Chem. Commun.* **1997**, 193−194.
(10) Weyermann, P.; Gisselbrecht, J. P.; Boudon, C.; Diederich, F.; Gross, M. *Angew. Chem., Int. Ed. Engl.* **1999**, *38*, 3215−3219.
(11) Van Doorslaer, S.; Zingg, A.; Schweiger, A.; Diederich, F. *ChemPhysChem* **2002**, *3*, 659−667.
(12) Gorman, C. B. *Adv. Mater.* **1997**, *9*, 1117−1119.
(13) Tyler, T. L.; Hanson, J. E. *Chem. Mater.* **1999**, *11*, 3452−3459.
(14) Weintraub, J. G.; Parquette, J. R. *J. Org. Chem.* **1999**, *64*, 3796−3797.
(15) Harth, E. M.; Hecht, S.; Helms, B.; Malmstrom, E. E.; Fréchet, J. M. J.; Hawker, C. J. *J. Am. Chem. Soc.* **2002**, *124*, 3926−3938.
(16) Trollsås, M.; Atthof, B.; Würsch, A.; Hedrick, J. L.; Pople, J. A.; Gast, A. P. *Macromolecules* **2000**, *33*, 6423−6438.
(17) Percec, V.; Cho, W. D.; Ungar, G.; Yeardley, D. J. P. *J. Am. Chem. Soc.* **2001**, *123*, 1302−1315.
(18) Li, S.; McGrath, D. V. *J. Am. Chem. Soc.* **2000**, *122*, 6795−6796.
(19) Hayakawa, J.; Momotake, A.; Arai, T. *Chem. Commun.* **2003**, 94−95.
(20) Archut, A.; Vögtle, F.; DeCola, L.; Azzellini, G. C.; Balzani, V.; Ramanujam, P. S.; Berg, R. H. *Chem. Eur. J.* **1998**, *4*, 699−706.
(21) Archut, A.; Azzellini, G.; Balzani, V.; De Cola, L.; Vögtle, F. *J. Am. Chem. Soc.* **1998**, *120*, 12187−12191.
(22) Junge, D.; McGrath, D. *J. Am. Chem. Soc.* **1999**, *121*, 4912−4913.
(23) Tsuda, K.; Dol, G. C.; Gensch, T.; Hofkens, J.; Latterini, L.; Weener, J. W.; Meijer, E. W.; De Schryver, F. C. *J. Am. Chem. Soc.* **2000**, *122*, 3445−3452.

10.1021/ja035515f CCC: $25.00

the relative rates of photoinduced, intramolecular electron transfer of constitutional isomers of a triphenylamine core dendrimer substituted with a peryleneimide acceptor at the periphery were probed.[27] Ideal dendrimer isomers differ only in their primary structure. Changes in the primary structure of the dendrimer can result in a change in its conformation (e.g., the disposition of the arms around the core and the relative degree to which the core is buried in the dendrimer). This change in conformation could be reflected in a change in the measured degree of encapsulation of the core. For example, in the case of an electroactive core (such as is discussed here), a change in the kinetics and/or thermodynamics of electron transfer to/from that core is expected.

What primary structural elements in dendrimers are most effective at influencing the conformation of these molecules? Several notable efforts have elucidated structure−property relationships by changing the primary structure of the dendrons to bias dendrimer conformation.[14,28−30] Conformation can be biased by a number of factors including the relative degree of solvation, the presence of internal hydrogen-bonding sites,[31−34] and steric factors including chiral moieties within the primary structure.[18,35−43]

We and others[36,37,44−49] have hypothesized that primary structural elements that create backfolded linkages within the dendrimer should increase the degree of steric congestion around the core moiety of the dendrimer. This behavior should lead to more effective encapsulation. To probe this hypothesis experimentally, three pairs of constitutional isomeric dendrimers (Figure 1) were synthesized and studied. These molecules allow the direct comparison of extended and backfolded architecture independent of the molecular weight. Here, several computational and experimental sets of data are presented to support the conclusion that backfolded linkages in a dendrimer result in more effective encapsulation of its core.

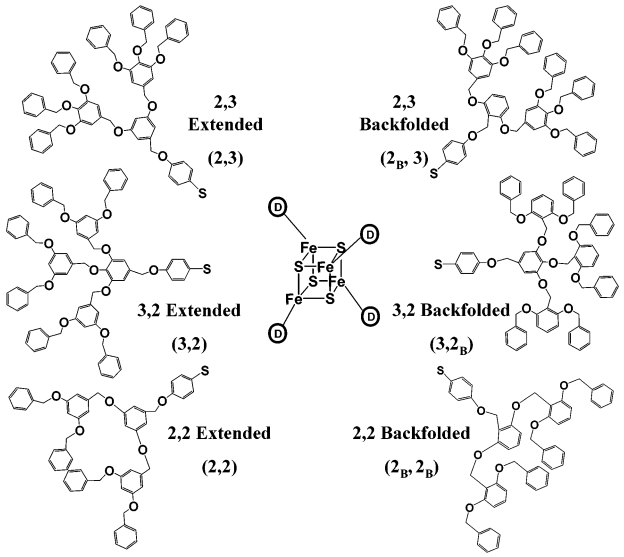

Figure 1. Structures of the constitutional isomeric dendrimer pairs. Each dendrimer has the form $(n\mathrm{Bu}_4)_2[\mathrm{Fe}_4\mathrm{S}_4\mathrm{D}_4]$, where D indicates a dendron substituted with a focal aromatic thiol. For each molecule, four identical ligands are attached to the iron−sulfur core (denoted by a circled D).

Results and Discussion

A. Synthesis. Each dendrimer structure synthesized consisted of benzyl ether-based repeat units previously reported by Fréchet et al.[50] and Rosini et al.[46] Each dendrimer was synthesized using a convergent activate/couple approach. The six molecular structures are depicted in Figure 1. The extended and backfolded designations refer to the aromatic substitution patterns of the benzyl ether groups. Isomers containing 3,5-disubstituted linkages are designated as extended, while those containing 2,6-disubstituted linkages are referred to as backfolded. Dendrons focally substituted with aromatic thiols were synthesized as described in the Supporting Information (Schemes S1−S5). Several synthetic issues are of particular note. First, it was found that the thiol group could be efficiently protected and deprotected (with silver nitrate) using a tetrahydropyranyl (THP) group. The iron−sulfur cluster dendrimers were synthesized in good yields using ligand-exchange around $(n\mathrm{Bu}_4\mathrm{N})_2[\mathrm{Fe}_4\mathrm{S}_4(S\text{-}t\text{-}\mathrm{Bu})_4]$ as described previously.[5] In addition, care had to be taken with all molecules containing backfolded linkages due to their susceptibility to acid cleavage of the benzyl ether groups as detailed previously.[51,52] Reaction and purification steps had to be carried out in neutral or slightly basic conditions for these particular compounds. All activated (halogenated) intermediates were thus carried on without purification.

B. Computational Conformational Searching. Before committing to the synthesis of new molecules, it was of interest to determine, from computations, if a backfolded isomer would provide better encapsulation than its extended counterpart.

(24) Weener, J. W.; Meijer, E. W. *Adv. Mater.* **2000**, *12*, 741−746.
(25) Nagasaki, T.; Tamagaki, S.; Ogino, K. *Chem. Lett.* **1997**, 717−718.
(26) Newkome, G. R.; He, E.; Godinez, L. A.; Baker, G. R. *J. Am. Chem. Soc.* **2000**, *122*, 9993−10006.
(27) Lor, M.; Thielemans, J.; Viaene, L.; Cotlet, M.; Hofkens, J.; Weil, T.; Hampel, C.; Müllen, K.; Verhoeven, J. W.; Van der Auweraer, M.; De Schryver, F. C. *J. Am. Chem. Soc.* **2002**, *124*, 9918−9925.
(28) Percec, V.; Ahn, C.-H.; Ungar, G.; Yeardley, D. J. P.; Möller, M.; Sheiko, S. S. *Nature* **1998**, *391*, 161−164.
(29) Percec, V.; Chu, P.; Ungar, G.; Zhou, J. *J. Am. Chem. Soc.* **1995**, *117*, 11441−11454.
(30) Balagurusamy, V. S. K.; Ungar, G.; Percec, V.; Johansson, G. *J. Am. Chem. Soc.* **1997**, *119*, 1539−1555.
(31) Sijbesma, R. P.; Beijer, F. H.; Brunsveld, L.; Folmer, B. J. B.; Hirschberg, J. H. K. K.; Lange, R. F. M.; Lowe, J. K. L.; Meijer, E. W. *Science* **1997**, *278*, 1601−1604.
(32) Ma, Y. G.; Kolotuchin, S. V.; Zimmerman, S. C. *J. Am. Chem. Soc.* **2002**, *124*, 13757−13769.
(33) Elizarov, A. M.; Chang, T.; Chiu, S. H.; Stoddart, J. F. *Org. Lett.* **2002**, *4*, 3565−3568.
(34) Zimmerman, S. C.; Zeng, F.; Reichert, D. E. C.; Kolotuchin, S. V. *Science* **1996**, *271*, 1095−1098.
(35) Laufersweiler, M. J.; Rohde, J. M.; Chaumette, J. L.; Sarazin, D.; Parquette, J. R. *J. Org. Chem.* **2001**, *66*, 6440−6452.
(36) Gandhi, P.; Huang, B. H.; Gallucci, J. C.; Parquette, J. R. *Org. Lett.* **2001**, *3*, 3129−3132.
(37) Recker, J.; Tomcik, D. J.; Parquette, J. R. *J. Am. Chem. Soc.* **2000**, *122*, 10298−10307.
(38) Higashi, N.; Koga, T.; Niwa, M. *Adv. Mater.* **2000**, *12*, 1373−1375.
(39) Pugh, V. J.; Hu, Q. S.; Pu, L. *Angew. Chem., Int. Ed. Engl.* **2000**, *39*, 3638−3641.
(40) Lellek, V.; Stibor, I. *J. Mater. Chem.* **2000**, *10*, 1061−1073.
(41) Chow, H.-F.; Mak, C. C. *Pure Appl. Chem.* **1997**, *69*, 483−488.
(42) Junge, D. M.; Wu, M. J.; McElhanon, J. R.; McGrath, D. V. *J. Org. Chem.* **2000**, *65*, 5306−5314.
(43) McElhanon, J. R.; McGrath, D. V. *J. Org. Chem.* **2000**, *65*, 3525−3529.
(44) Peerlings, H. W. I.; Trimbach, D. C.; Meijer, E. W. *Chem. Commun.* **1998**, 497−498.
(45) Percec, V.; Cho, W. D.; Möller, M.; Prokhorova, S. A.; Ungar, G.; Yeardley, D. J. P. *J. Am. Chem. Soc.* **2000**, *122*, 4249−4250.
(46) Rosini, C.; Superchi, S.; Peerlings, H. W. I.; Meijer, E. W. *Eur. J. Org. Chem.* **2000**, 61−71.
(47) Huang, B. H.; Parquette, J. R. *J. Am. Chem. Soc.* **2001**, *123*, 2689−2690.
(48) Peng, Z. H.; Pan, Y. C.; Xu, B. B.; Zhang, J. H. *J. Am. Chem. Soc.* **2000**, *122*, 6619−6623.
(49) Percec, V.; Cho, W. D.; Ungar, G.; Yeardley, D. J. P. *Chem. Eur. J.* **2002**, *8*, 2011−2025.
(50) Hawker, C. J.; Fréchet, J. M. J. *J. Am. Chem. Soc.* **1990**, *112*, 7638−7647.
(51) Percec, V.; Cho, W. D.; Mosier, P. E.; Ungar, G.; Yeardley, D. J. P. *J. Am. Chem. Soc.* **1998**, *120*, 11061−11070.
(52) Peerlings, H. W. I.; Trimbach, D. C.; Meijer, E. W. *Chem. Commun.* **1998**, 497−498.

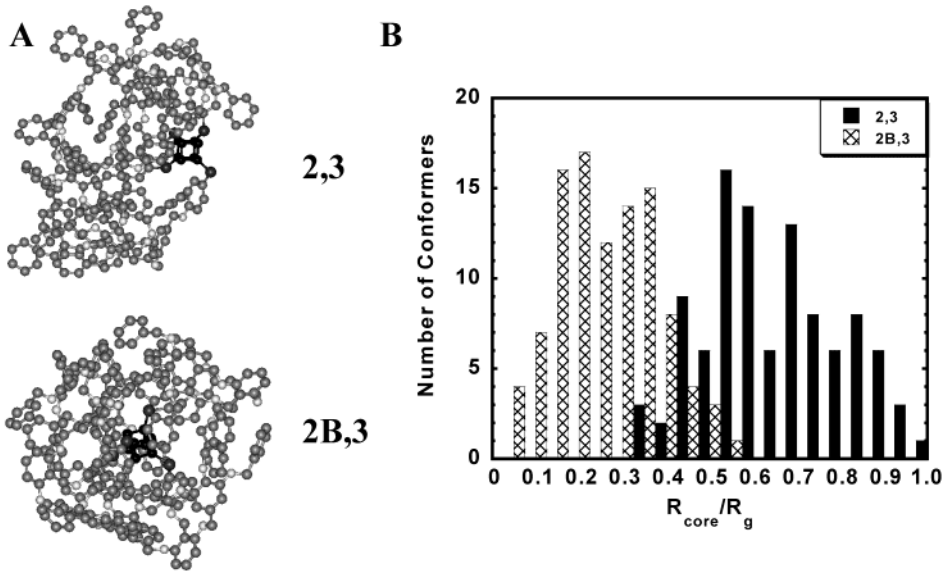

Figure 2. (A) Ball and stick figures of the lowest energy conformers of models of the molecules 2,3 and 2_B,3 found during a conformational search of each. (B) Histogram counting the number of conformers found at an energy minimum and with a given core displacement ($R_{core}/R_g = 0$ for core at center, $R_{core}/R_g = 1$ for core at edge).

Previously, we showed that the conformational manifold of dendrimers could be sketched using high-temperature, quenched molecular dynamics. Using such a conformational search protocol, the relative molecular size and displacement of the core within a dendrimer could be examined.[5] This technique was applied to study models of two of the dendrimer isomers—the molecules labeled 2,3 and 2_B,3 in Figure 1. In Figure 2, two types of data are shown that resulted from a conformational search that tabulated 100 minimum energy structures for each of these molecular models. Figure 2A shows ball-and-stick models of the lowest energy conformations of each of the dendrimer models. Figure 2B shows a histogram illustrating the distribution of core positions for each of the dendrimer models. The value R_{core} is the distance from the center of mass to the center of the iron−sulfur cluster and R_g is the computed radius of gyration of the model. A ratio of R_{core}/R_g of zero finds the core at the center of mass of the dendrimer model. As this ratio increases, the core is found more and more offset from the center of mass of the model.

Both the snapshot conformations and the conformational distributions shown in Figure 2 indicate more efficient encapsulation in the backfolded molecule compared to the extended isomer. Although snapshots from molecular dynamics are somewhat misleading, as they indicate only a moment in time for a dynamic structure, one can employ them to see easily that the backfolded isomer encapsulates the core more efficiently than the extended isomer. In a statistically more relevant way, the histogram shows, on average, a greater relative core offset for the extended dendrimer architecture indicative of a mobile core that resides toward the outer part of the dendrimer. Conversely, the histogram of the backfolded architecture shows a core that is, on average, more centrally located within the molecule. These observations are thus consistent with the hypothesis that the 2,6-benzyl substitution pattern results in a backfolded, more compact dendrimer where the core resides toward the center of the molecule as compared to the isomer with a 3,5-benzyl substitution pattern.

C. Determination of Redox Potential and Heterogeneous Electron-Transfer Rate Constants. Given the hypothesis that backfolding leads to more effective encapsulation, two major effects on the electrochemical behavior of the dendrimer isomers are predicted. First, it is expected that the iron−sulfur cluster will be more difficult to reduce as it is encapsulated in a dendrimer microenvironment that is more hydrophobic than the solvent. This type of redox potential shift has been observed in a number of iron−sulfur cluster proteins and mutants[53−62] and in small molecule models.[63−67] Moreover, the rate constant for heterogeneous electron transfer is expected to be lower in the backfolded molecules compared to the extended isomers. As illustrated below, both of these effects were prominent in the comparison of the redox behavior of dendrimer isomers. To our knowledge, no experiments have been reported to probe the

(53) Iismaa, S. E.; Vazquez, A. E.; Jensen, G. M.; Stephens, P. J.; Butt, J. N.; Armstrong, F. A.; Burgess, B. K. *J. Biol. Chem.* **1991**, *266*, 21563−21571.
(54) Chen, K. S.; Tilley, G. J.; Sridhar, V.; Prasad, G. S.; Stout, C. D.; Armstrong, F. A.; Burgess, B. K. *J. Biol. Chem.* **1999**, *274*, 36479−36487.
(55) Chen, K. S.; Jung, Y. S.; Bonagura, C. A.; Tilley, G. J.; Prasad, G. S.; Sridhar, V.; Armstrong, F. A.; Stout, C. D.; Burgess, B. K. *J. Biol. Chem.* **2002**, *277*, 5603−5610.
(56) Chen, K. S.; Bonagura, C. A.; Tilley, G. J.; McEvoy, J. P.; Jung, Y. S.; Armstrong, F. A.; Stout, C. D.; Burgess, B. K. *Nat. Struct. Biol.* **2002**, *9*, 188−192.
(57) Low, D. W.; Hill, M. G. *J. Am. Chem. Soc.* **2000**, *122*, 11039−11040.
(58) Shen, B. H.; Jollie, D. R.; Stout, C. D.; Diller, T. C.; Armstrong, F. A.; Gorst, C. M.; La Mar, G. N.; Stephens, P. J.; Burgess, B. K. *J. Biol. Chem.* **1994**, *269*, 8564−8575.
(59) Capozzi, F.; Ciurli, S.; Luchinat, C. In *Structure and Bonding: Metal Sites in Proteins and Models*; Hill, H. A. O., Sadler, P. J., Thompson, A. J., Eds.; Springer-Verlag: Berlin, 1998; Vol. 90, pp 127−160.
(60) Soriano, A.; Li, D. W.; Bian, S. M.; Agarwal, A.; Cowan, J. A. *Biochemistry* **1996**, *35*, 12479−12486.
(61) Langen, R.; Jensen, G. M.; Jacob, U.; Stephens, P. J.; Warshel, A. *J. Biol. Chem.* **1992**, *267*, 25625−25627.
(62) Jensen, G. M.; Warshel, A.; Stephens, P. J. *Biochemistry* **1994**, *33*, 10911−10924.
(63) Hill, C. L.; Renaud, J.; Holm, R. H.; Mortenson, L. E. *J. Am. Chem. Soc.* **1977**, *99*, 2549−2557.
(64) Martens, C. F.; Bongers, M. M. G.; Kenis, P. J. A.; Czajka, R.; Feiters, M. C.; Van der Linden, J. G. M.; Nolte, R. J. M. *Chem. Ber./Recl.* **1997**, *130*, 23−33.
(65) Tanaka, K.; Tanaka, T.; Kawafune, I. *Inorg. Chem.* **1984**, *23*, 516−518.
(66) Kuroda, Y.; Sasaki, Y.; Shiroiwa, Y.; Tabushi, I. *J. Am. Chem. Soc.* **1988**, *110*, 4049−4050.
(67) Okuno, Y.; Uoto, K.; Yonemitsu, O.; Tomohiro, T. *J. Chem. Soc., Chem. Commun.* **1987**, 1018−1020.

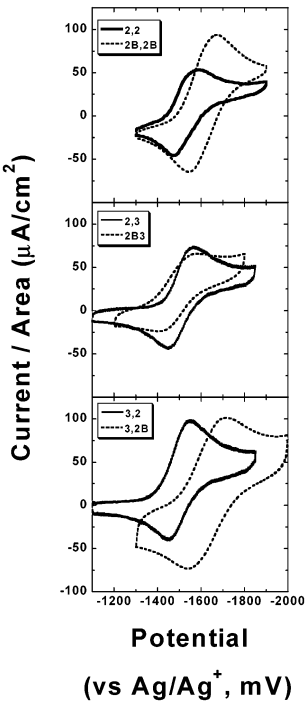

Figure 3. Cyclic voltammograms of each dendrimer isomer pair (1 mM dendrimer, 100 mM TEAF in DMF, scan rate of 50 mV/s).

effect of this type of conformational bias on the properties of an electroactive core.

Both cyclic voltammetry (CV) and Osteryoung square wave voltammetry (OSWV) were used to probe the electrochemical properties of the dendrimer samples. Cyclic voltammetry was used to determine redox potential ($E_{1/2}$) and peak separation (ΔE_p). Using diffusion coefficients obtained from chronoamperometry (see below) and a Nicholson analysis,[68] the heterogeneous electron-transfer rate constants (k_0) for a quasireversible system were calculated. This technique relates ΔE_p to the electron transfer rate constant of the sample in solution and is relatively accurate for quasi-reversible systems. CV also easily shows how rate and driving force vary for each isomer pair (Figure 3). However, at very fast and slow electron-transfer regimes, CV is limited as evidenced by the large relative error bars on these values. Thus, Osteryoung square wave voltammetry was used to determine accurate electron-transfer rate constants for each dendrimer, as it is useful particularly in the slow rate regime.

The redox potential and heterogeneous electron-transfer rate constants determined by CV and OSWV are given in Table 1. For each isomer pair, the backfolded architecture results in a more negative redox potential compared to the extended architecture. This behavior is consistent with encapsulation of the cluster in a more hydrophobic, less solvent-accessible microenvironment. This hypothesis is further supported by the observation that the rate constant for electron transfer of each of the backfolded dendrimers was slower compared to its extended counterpart.

D. Molecular Size and Its Relation to Electron-Transfer Rate. Diffusion coefficients (D_0) for the molecules were required to calculate heterogeneous electron-transfer rate constants given a freely diffusing model. This model was validated by verifying that peak current was proportional to the square root of the scan rate (Figure S2). In addition, diffusion coefficients can be used to measure the effective size of the molecules in solution. The diffusion coefficient for each molecule was determined using the two complementary techniques of chronoamperometry (CA) and pulsed field gradient spin−echo ^{1}H NMR (PFGSE) using methodology described previously.[5] These data are given in Table 1. The hydrodynamic radii (R_H) of the molecules were computed from these values using the Stokes−Einstein equation. The radii of the backfolded dendrimers, in each case, were smaller compared to the extended architectures.

It is perhaps intuitive that the backfolding of the dendrons in toward the core would result in a smaller more compact structure. However, why does the electron-transfer rate become slower for the smaller dendrimers? At first glance, this result seems counterintuitive given the likelihood that electron transfer occurs via tunneling through the dendrimer, the rate of which should be governed by distance. Figure 4 illustrates how a smaller molecule could have a larger effective electron-transfer distance. It suggests that if the mobility of the redox-active core around the center of mass of the molecule was lower, the effective distance of electron transfer would increase. The outer circle in each model denotes the hydrodynamic radius of each dendrimer. The darker, inner region suggests relative core mobility within the dendrimer. The width of the outer white segment can be considered as the effective electron-transfer distance. The computational results as well as the T_1 relaxation values presented below both support the contention that the extended architectures are more flexible than the backfolded architectures, allowing for greater movement of the core throughout the dendrimer. The backfolded architectures sterically hinder the core, keeping it closer to the center of the dendrimer. This steric hindrance causes a decrease in overall molecular size but an increase in effective electron-transfer distance.

E. Further Probing of Size and Mobility via NMR Relaxation Measurements. We previously showed that the paramagnetic nature of the Fe_4S_4 core of the dendrimer could be used to evaluate the relative proximity of various sets of chemically equivalent nuclei with respect to the core. To the extent that the protons on the dendron arms and the core interact closely, the longitudinal relaxation time constant (T_1) of these nuclei is expected to decrease. This interaction is consistent with steric congestion around the iron−sulfur core. Figure 5 compares the T_1 values obtained for the terminal aromatic proton signals (e.g., $C_6\mathbf{H}_5CH_2O$) for each dendrimer isomer. The terminal protons were chosen as their NMR signal was well resolved from all others, and they represent the topologically most distant point from the core of the dendrimer. Therefore, changes in the relaxation behavior of these protons between isomers indicates backfolding toward the molecular core.

In each case, the T_1 values for the backfolded isomer were shorter than those for the extended isomer. This behavior is consistent with a steric bias in the backfolded architectures resulting in a conformation that creates a smaller, more compact dendrimer compared to the extended architectures. The relative decrease in T_1 value between the backfolded and extended isomer also paralleled the molecular sizes obtained from PFGSE-NMR and chronoamperometry. Specifically, the difference was largest between the extended, 2,2 dendrimer and the backfolded

(68) Nicholson, R. S. *Anal. Chem.* **1965**, *37*, 1351−1355.

Table 1. Diffusion Coefficients, D_0, Obtained from Pulsed Field Gradient Spin−Echo NMR Spectroscopy (PFGSE) and Chronoamperometry (CA), Corresponding Stokes−Einstein Radius, R_H, Heterogeneous Electron-Transfer Rate Constant (k_0), Reduction Potential ($E_{1/2}$), and Transfer Coefficient (α) for the One-Electron Redox Couple $[Fe_4S_4(S\text{-Dend})_4]^{2-/3-}$

	PFGSE- NMR		CA		CV		OSWV		
structu re[a]	D_0 ($\times 10^6$ cm^2/s)	R_H (Å)[b]	D_0 ($\times 10^6$ cm^2/s)	R_H (Å)[b]	k_0 ($\times 10^3$ cm/s)	$E_{1/2}$ (mV)	k_0 ($\times 10^3$ cm/s)	$E_{1/2}$ (mV)	α
2,3	2.16(0.03)[c]	14.94(0.21)	3.01(0.19)	10.72(0.26)	2.95(0.93)	−1514(4)	2.34(0.44)	−1500(4)	0.44(0.02)
2B,3	2.57(0.07)	12.55(0.35)	3.26(0.10)	9.90(0.18)	1.11(0.15)	−1519(7)	0.92(0.34)	−1513(5)	0.50(0.02)
3,2	2.43(0.02)	13.28(0.11)	2.78(0.05)	11.86(0.34)	3.88(0.71)	−1494(4)	3.94(0.67)	−1498(3)	0.48(0.03)
3,2B	5.09(0.07)	5.44(0.09)	4.26(0.17)	7.58(0.18)	1.94(0.62)	−1623(7)	0.67(0.19)	−1606(12)	0.50(0.003)
2,2	2.68(0.05)	12.04(0.23)	2.81(0.10)	11.51(0.35)	3.86(0.88)	−1519(5)	1.58(0.45)	−1516(2)	0.37(0.02)
2B,2B	5.98(0.06)	5.40(0.06)	5.88(0.16)	5.50(0.33)	2.55(0.81)	−1614(1)	0.45(0.48)	−1589(2)	0.48(0.006)

[a] As shown in Figure 1. [b] Hydrodynamic radius calculated using the Stokes−Einstein equation. [c] Values in parentheses represent 90% confidence intervals of the values found.

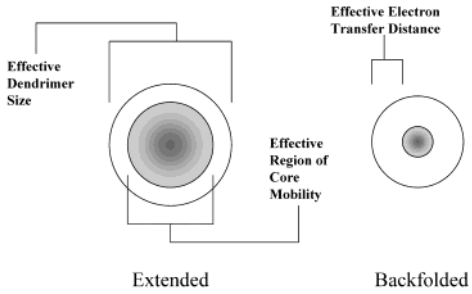

Figure 4. Cartoon illustrating the role of core mobility and molecular size on the effective electron-transfer distance.

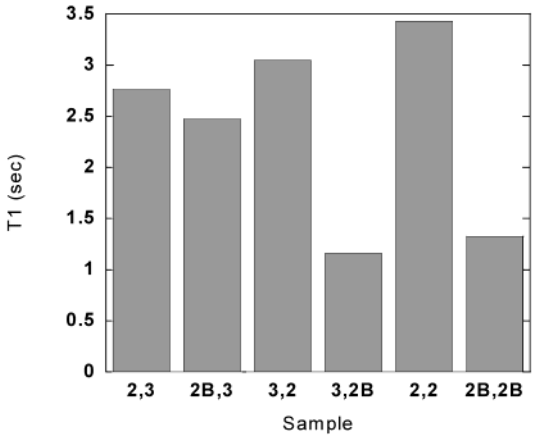

Figure 5. Bar graph indicating the relative T_1 values of terminal aromatic protons measured for each dendrimer (0.1 mM DMF solution).

2_B,2_B dendrimer. This result is not surprising as two generations of backfolding should result in the largest steric bias. In contrast, the 2,3/2_B,3 isomer pair showed the smallest difference in T_1 values. Again, this result was not unexpected since the backfolding linkages of this molecule were within the first generation. The linkages in the second generation were plausibly not sterically restricted and remained capable of extending out from the core. Thus, these nuclei interacted less with the iron−sulfur cluster.

It should be noted that the trends in T_1 cannot be explained by differences in the relative rotation or diffusion rates of the molecules. These molecules showed an increase in T_1 with increasing temperature and thus were in the "liquid-like" regime where the internuclear vectors (or electron−nuclear vector) oscillate at greater than the Larmor frequency.[6] Thus, based only on relative rotation rates (e.g., only the rate of tumbling of the entire molecule in solution), smaller molecules should have larger T_1 values. The opposite was observed here, indicating that differences in the degree of paramagnetic relaxation, not nuclear dipole−dipole relaxation, explains the differences observed.

Conclusions

Dendrimer conformation can be biased by primary structural elements in ways that manifest themselves in the measured degree of core encapsulation. Using a combination of electrochemical, NMR, and computational methods, a consistent set of data were obtained to support the conclusion that backfolded linkages result in dendrimers that are more encapsulating yet smaller than their extended counterparts. This conclusion was made by direct comparison of sets of dendrimer isomers that differed only in this relative structural element. Encapsulation behaviors manifested as predicted changes in both rate and driving force for electron transfer. In rationalizing this behavior, one must consider the effective distance of electron transfer and not just molecular size. This effective distance depends on both molecular size and the relative mobility of the redox-active core within the molecule.

Acknowledgment. This work was supported in part by the Graduate Assistance in Areas of National Need Electronic Materials fellowship and the National Science Foundation (NSF CHE-9900072). We thank Hanna Sierzputowska-Gracz for assistance in collecting PFGSE data. We acknowledge the North Carolina Supercomputer Center for computational resources. Mass spectra were obtained at the Mass Spectrometry Laboratory for Biotechnology. Partial funding for the facility was obtained from the North Carolina Biotechnology Center and the National Science Foundation.

Supporting Information Available: Cyclic voltammetry and Osteryoung square wave voltammetry data; details of the synthesis of each dendrimer, characterization information, and synthetic schematics. This material is available free of charge via the Internet at http://pubs.acs.org. See any current masthead page for ordering information and Web access instructions.

JA035515F